Illuminating Single Molecules in Condensed Matter

W. E. Moerner[1] and Michel Orrit[2]

Efficient collection and detection of fluorescence coupled with careful minimization of background from impurities and Raman scattering now enable routine optical microscopy and study of single molecules in complex condensed matter environments. This ultimate method for unraveling ensemble averages leads to the observation of new effects and to direct measurements of stochastic fluctuations. Experiments at cryogenic temperatures open new directions in molecular spectroscopy, quantum optics, and solid-state dynamics. Room-temperature investigations apply several techniques (polarization microscopy, single-molecule imaging, emission time dependence, energy transfer, lifetime studies, and the like) to a growing array of biophysical problems where new insight may be gained from direct observations of hidden static and dynamic inhomogeneity.

In the final decades of this century, much scientific research has turned toward the dream voiced by Richard Feynman in 1959 to manipulate and control matter on an atomic and molecular scale (*1*). Attaining the ultimate limit of probing single molecules and atoms and subsequently modifying their behavior has been a primary goal. Highly successful approaches to exploring single atoms or molecules on surfaces have used nanometer-scale interactions with tunneling electrons or forces from sharp tips, in scanning tunneling microscopy (STM) (*2*) or atomic force microscopy (AFM) (*3*). On the other hand, optical probing of single quantum systems offers the advantage of "operation at a distance," which can result in smaller perturbations of the object under study but may be accompanied by a potential loss in spatial resolution. Important early advances involved the optical spectroscopy of single electrons or ions confined in electromagnetic traps, with which many fundamental physical predictions were confirmed (*4*).

We focus on the optical probing of single molecules, atoms, or ions in complex condensed matter environments, a regime which presents significant challenges as well as exciting opportunities for discovery. The challenges generally derive from the limitations posed by diffraction effects and the difficulty of detecting a single entity in the interfering background arising from the host crystal, polymer, liquid, or protein. The opportunities result from the wealth of new information obtainable regarding the interactions of the single entity with its native environment, unobscured by the ensemble averaging that characterizes conventional experiments. Although the ideas we present can be applied to molecules, or atoms, or ions, the principal thrust of recent work has been on single molecules, chiefly because of signal-to-noise considerations.

Why is it useful to study individual molecules in a complex condensed matter host, each of which may be marching to the beat of a different drummer? Clearly, standard ensemble measurements that yield the average value of a parameter for a large number of (presumably identical) copies of the system of interest still have great value. By contrast, single-molecule measurements completely remove the ensemble averaging. Of course, workers in this field never report the results from only one single molecule, but rather from many single molecules, one by one. This allows construction of a frequency histogram of the actual distribution of values for an experimental parameter, rather than just the average (mean) value of the distribution. All would agree that the distribution contains more information than the average value alone. The shape of the full distribution can be examined to see whether there are multiple peaks, or whether it has a strongly skewed shape. These details of the underlying distribution become crucially important when the system under study is inhomogeneous. This would be expected to be the case for many complex condensed matter environments. Fortunately, a single molecule can be viewed as a local reporter of its "nanoenvironment," that is, the exact constellation of functional groups, atoms, ions, electrostatic charges, or other sources of local fields in its immediate vicinity. For biomolecules, heterogeneity easily arises, for example, if the various individual copies of a protein or oligonucleotide are in different folded states or different configurations.

Another reason for performing optical experiments in the single-molecule regime is that they remove the need for synchronization of many single molecules undergoing a time-dependent process. For example, a large ensemble of molecules undergoing intersystem crossing events must be synchronized in order to measure the triplet lifetime. In the single-molecule regime, intersystem crossing becomes a digital, "yes or no" process, the observation of which has been termed "quantum jumping" as the system undergoes transitions from triplet state to singlet state and vice versa (*5*). Similar remarks apply to an enzymatic system that can be in one of several catalytic states. For the ensemble measurements, synchronization is required (and is often difficult), whereas if individuals are observed, any one member of the ensemble is in only one state at a given time, and thus the specific sequence of binding, hydrolysis, and other catalytic steps is available for study.

A final reason for the use of single-molecule techniques is the possibility of observing new effects in unexplored regimes. For example, some single-molecule systems have unexpectedly shown some form of fluctuating, flickering, or stochastic behavior. The absorption frequency of the single molecule can change as a result of a change in its photophysical parameters or a change in local environment; this behavior has been termed "spectral diffusion." If a fixed-frequency laser is used to probe a spectrally diffusing molecule, the shifting of the absorption in and out of resonance generates amplitude fluctuations in the detected emission signal, which can be analyzed to gain knowledge about the underlying physical mechanism. Such fluctuations are now becoming important diagnostics of the single-molecule regime, and they provide unprecedented insight into behavior which is generally obscured by ensemble averaging. Several comprehensive reviews of this area may be consulted for details beyond the scope of this article (*6*–*11*).

General Principles and Methods

The daunting task of detecting a single absorbing molecule amidst trillions of nominally transparent solvent or matrix molecules requires two deceptively simple steps: (i) establishing that only one molecule in the irradiated volume is in resonance with the laser, and (ii) ensuring that the signal from the single molecule is larger than that from any interfering background signal. The first optical studies of a single molecule involved a sophisticated laser absorption technique insensitive to sample scattering (*12*); however, ultrasensitive fluorescence techniques have been shown to produce higher signal-to-noise when sample back-

[1]Department of Chemistry, Stanford University, Stanford, CA 94305–5080, USA. [2]Centre de Physique Moléculaire Optique et Hertzienne, UMR 5798, CNRS and Université Bordeaux I, 33405 Talence, France.

E-mail: w.e.moerner@stanford.edu (W.E.M.); orrit@yak.cpmoh.u-bordeaux.fr (M.O.)

grounds are carefully controlled (*13*). Fluorescence emission usually represents only a tiny fraction of the incident energy, but gives rise to emitted photons that are red-shifted with respect to the excitation. These photons can be efficiently sifted out of an overwhelming number of photons in the exciting beam, so that the signal of a single molecule can be detected with a high signal-to-background ratio. The physical mechanism leading to fluorescence (that is, to a red shift of the emitted photon) may be described with reference to the electronic energy levels of a prototypical molecule in Fig. 1. After the absorption of an exciting photon (λ_{RT} for example), the excited molecule quickly relaxes by generation of vibrational modes of the molecule and the host (phonons) to the lowest electronic excited state, from which fluorescence photons can be emitted (dashed lines). After the emission, the molecule is brought back to the initial ground state by further vibrational and phonon relaxation, and the partitioning between the various colors of emission is controlled by the well-known Franck-Condon and Debye-Waller factors expressing the extent of vibrational relaxation and electron-phonon coupling, respectively. In general, the relaxation steps represent energy losses which cause a spectral red shift between absorption and emission bands, called the Stokes shift. Polycyclic aromatic hydrocarbons, for example, are rigid molecules for which the Stokes shift is often small (less than 1000 cm^{-1}). In a frozen environment at low temperature, their geometry change (relaxation) can be so small that a very narrow line appears in the absorption and fluorescence spectrum. This rearrangement-free optical line is known as the zero-phonon line and is used in many optical experiments at cryogenic temperatures (*9*). Dye molecules, on the other hand, are widely used for fluorescence experiments at room temperature (*11, 14*). They often undergo large rearrangements of their charge distribution upon excitation, leading to much larger Stokes shifts (about 1500 cm^{-1} for rhodamine dyes, 6000 cm^{-1} for DCM, a well-known laser dye). In discussing single-molecule fluorescence, two important quantities must be considered, namely the rate of fluorescence and the total energy or number of photons that a molecule can emit on average. In the case of organic molecules, the rate is often limited by trapping in a dark state, such as the triplet state example of Fig. 1, where absorption and fluorescence are switched off. Efficient fluorophores like laser dyes which have small values of k_{ISC} or short lifetimes of the dark states (large k_T), or both, will be easiest to detect. The total amount of fluorescence per molecule is limited in ambient conditions to roughly 10^6 photons by photobleaching, that is, by photochemical reactions in the excited state which irreversibly alter the chemical structure of the fluorophore. At cryogenic temperatures, photodecomposition channels are often suppressed, and small reactive molecules such as oxygen or water are frozen and cannot diffuse. Then, the amount of fluorescence is limited only by sudden conformational changes of the host-guest system, which shift the absorption line of the molecule away from resonance with the laser. For some crystal systems at low temperatures, the available amount of fluorescence per molecule can be virtually infinite (*9*).

The selection of single emitting objects in condensed matter is not restricted to organic molecules. Defects in insulating materials such as color centers (a class of defects including electrons loosely bound to vacancies), transition metal ions, or rare earth ions have fluorescence mechanisms similar to that of molecules. Although a clear signal from a single impurity ion has yet to be demonstrated, single nitrogen-vacancy color centers in diamond have been detected and investigated (*15*). Small semiconductor nanocrystals, known as quantum dots, can form spontaneously during the growth of semiconductor heterostructures or be prepared chemically in solution. Researchers started to detect single quantum dots optically several years ago and are currently investigating their spectroscopic and photochemical properties (*16*). Nanoparticles range from 2 to 10 nm in diameter, whereas islands in heterostructures have sizes of a few tens of nanometers. Quantum dots are thus considerably larger than a laser dye molecule, and the mechanism of their emission therefore involves several electronic states, making it more complex than that of a typical fluorophore. Quantum dots are highly resistant to photobleaching, and they might be used instead of molecules in many applications, for example in cytometry and immunocytobiology, where large amounts of fluorescence are required from each single emitter (*17*).

Single-molecule fluorescence signals are rather weak and can easily be drowned in background and noise. For ease in detection of single molecules, experimentalists must choose the right compound. In order to optimize the emission rate, the probe molecules should possess a strongly allowed absorption transition and a high fluorescence yield. An important parameter characterizing the interaction of a molecule with light is the absorption cross-section, which may be regarded as the effective "area" of the molecule for "capture" of an incoming photon. The general expression for the cross-section for a randomly oriented molecule is $\sigma = 2\pi(\lambda/2\pi)^2 (\gamma_r/\Gamma_{tot})$, where λ is the light wavelength, γ_r the spontaneous (that is, radiative) fluorescence rate, and Γ_{tot} the total frequency width of the absorption (*9, 18*). For a dye molecule in solution at room temperature, γ_r is about 10^{-3} cm^{-1}, which corresponds to a radiative lifetime of a few nanoseconds, and Γ_{tot} is about 1000 cm^{-1}, so that the absorption cross-section of a single dye molecule is $\sigma \sim 6$ $Å^2$, a value comparable to the molecular size. For the zero-phonon line of an aromatic molecule at low temperature, the linewidth is dramatically smaller, about $\Gamma_{tot} = 10^{-3}$ cm^{-1}, and the radiative rate of the zero-phonon line is reduced from the total value at room temperature by the Debye-Waller factor (about 0.1). Therefore, the absorption cross-section is many orders of magnitude larger than at room temperature, up to about $\sigma = 10^6$ $Å^2$, corresponding to the total physical area of some 100,000 molecules! Another important parameter is the maximum emission rate of a molecule at very high excitation power when optical saturation occurs. For a two-level molecule, this rate is given by $\tau_f^{-1}/2$, and for a typical fluorescence lifetime τ_f of a strongly allowed transition of 5 ns, the emission rate reaches 10^8 s^{-1}. This value is sufficiently large that even with a modest detection efficiency, it is possible to have a very intense signal approaching millions of detected photons per second. Unfortunately, the rate is often limited by the bottleneck effect of dark states such as the triplet (Fig. 1), which reduces the maximum rate to $\tau_f^{-1}/(2 + k_{ISC}\tau_T)$, where k_{ISC} is the population rate of the dark state from the excited singlet and τ_T the lifetime of the dark state ($k_T = \tau_T^{-1}$ being its decay rate). For this reason, molecules with weak bottlenecks are generally preferred. The maximum photon emission rate also fixes the maximum time resolution of single-molecule studies to be in the nanosecond range, so that fluorescence lifetimes and other transient effects may be measured.

Despite the fact that single-molecule signals are relatively strong, struggling against all background sources is the foremost worry of experimentalists who work with single molecules. A first source of background may lie with experimental limitations such as the dark counts of the detector, the residual flu-

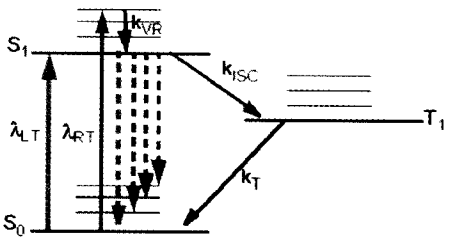

Fig. 1. Schematic representation of the electronic energy-level structure for single-molecule optical studies. S_0, ground singlet state; S_1, first excited singlet; T_1, lowest triplet state or other intermediate state. For each electronic state, several levels in the vibrational progression are shown. Typical low-temperature studies use wavelength λ_{LT} to pump the (0-0) transition, although at room temperature, shorter wavelengths λ_{RT} are more common. The intersystem crossing or intermediate production rate is k_{ISC}, and the intermediate decay rate is k_T. Fluorescence emission shown as dotted lines originates from S_1 and terminates on various vibrationally excited levels of S_0 (dotted red) or S_0 itself (dotted orange).

orescence from optical parts, particularly from colored glass filters, or residual emission by the excitation source in the spectral range where fluorescence is detected. But background photons emitted by the sample itself are more difficult to suppress. The two main sources are residual fluorescence from other impurities, and Raman scattering by the solvent or host matrix. Both are proportional to the volume of the illuminated sample. For example, a significant background in cryogenic experiments arises from phonon-assisted absorption by the other probe molecules. Even if their fluorescence yield is very weak, unwanted impurities or molecular components of the solvent, particularly in biological samples, can emit strong residual fluorescence. Residual fluorescence increases very rapidly with the energy of the exciting photon, and thus working in the blue or near-UV part of the spectrum will often give rise to more serious background problems. The total Raman scattering cross-section of a solvent molecule like benzene for one of its strongest modes is about 10^{-12} Å^2 (*7*), which gives a total cross-section of less than 10^{-2} Å^2 for an excited volume of 1 μm^3. This shows that Raman scattering is negligible for zero-phonon lines at cryogenic temperatures, but becomes comparable to the absorption cross-section of a single molecule in a solution at room temperature for excited volumes of about 100 μm^3.

Given that the background cross-sections are proportional to the excited volume, an optimal signal-to-background ratio will require a minimum excited volume. Various optical designs have been proposed to limit the excited volume (Fig. 2). By means of a lens or a single-mode optical fiber (Fig. 2A), a loosely focused excitation beam is obtained, which leads to volumes of the order of 100 μm^3. The tight focus of a microscope objective (Fig. 2B) illuminates a minimum volume of roughly 1 μm^3 due to diffraction effects, whereas subwavelength illumination through the small aperture of a near-field optical probe (Fig. 2C) gives volumes of about 10^{-2} μm^3 or less (*19*). Another useful detection configuration uses total internal reflection to reduce the illuminated volume (*20, 21*). A molecule radiates fluorescence photons in all directions of space, with the emission pattern of a dipole. To obtain a strong fluorescence signal, it is important to collect fluorescence over as wide a solid angle as possible. Several collection strategies have been used, for example parabolic mirrors or microscope objectives (Fig. 2). The same optical part can be used for excitation and collection. This is often the case in confocal designs, where the focal spot is imaged onto a small-area detector, usually a highly efficient avalanche photodiode (*22*).

To display data acquired for single molecules, it is useful to generalize the concept of an "image" beyond the conventional microscopic case in which the signal is displayed as a function of two spatial position variables (x and y). By displaying the signals from single molecules with their background as functions of a variety of control parameters, a generalized image is obtained in which the single molecules appear as discrete maxima or spots. To distinguish individual molecules in the image, their spots must not overlap. Therefore, the concentration must be so small that there is much less than one molecule on average in each image spot. The most straightforward control parameter is the spatial position on the sample (*19, 23*) (Fig. 3). This direct imaging method works best if the molecules do not diffuse too far during the recording time. In a conventional two- or three-dimensional image of the sample at room temperature, single molecules will appear as bright spots at different locations, provided c, the number density of molecules (or concentration), meets the requirement that $cV_{ill} \ll 1$, where V_{ill} is the illuminated volume. If the molecules move around, either by diffusion or because there is a flow of the liquid solution, the laser focus can be kept fixed inside the sample. Fluorescence bursts will then be observed whenever a single molecule crosses the focal spot (Fig. 4A) (*22, 24, 25*). These bursts are images of the single molecules in the time domain, with the same concentration requirement as above. To give another example, when either the excitation or the analysis device are scanned in wavelength at a fixed spot in the sample, the signals from single molecules also appear as "images" in the spectrum, whenever the homogeneous linewidth γ_{hom} of a single molecule line is much smaller than the inhomogeneous bandwidth Γ_{inh} of their distribution (Fig. 4B) (*9*). This method of spectral imaging is most useful at low temperatures, when the homogeneous width is small enough. The concentration requirement in this case is $cV_{ill} \ll \Gamma_{inh}/\gamma_{hom}$, much less stringent than for spatial or temporal imaging. The inhomogeneous broadening of the line is then exploited so as to efficiently reduce the concentration of resonant molecules in the sample. At room temperature, once the single-molecule limit has been achieved by spatial selection, spectral images can be obtained by dispersing the emission with a monochromator (*26*). Finally, various hybrid "images" can be formed, for example by using laser frequency as a control variable along one axis and position in the sample along another axis (Fig. 4C).

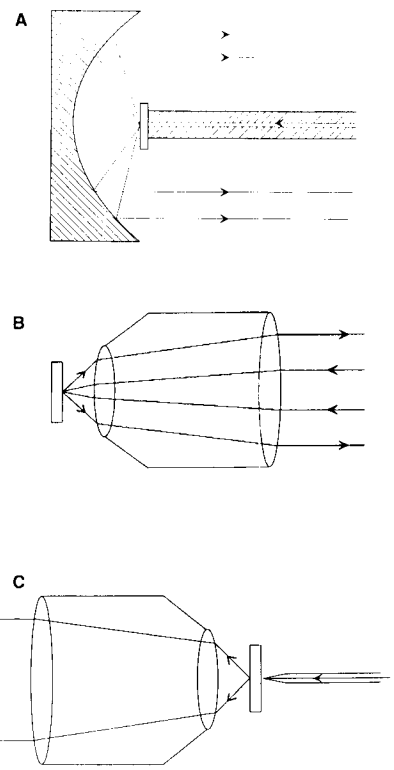

Fig. 2. Examples of optical designs used to select and detect single molecules. (**A**) Fiber-parabolic mirror, (**B**) microscope objective lens for excitation and fluorescence collection, (**C**) excitation by a pulled and metal-coated optical fiber and collection by an objective lens.

Overview of Results

Single-molecule spectroscopy at cryogenic temperatures. Because spectral lines of single molecules in solids at low temperatures are extremely narrow, often some tens of mega-

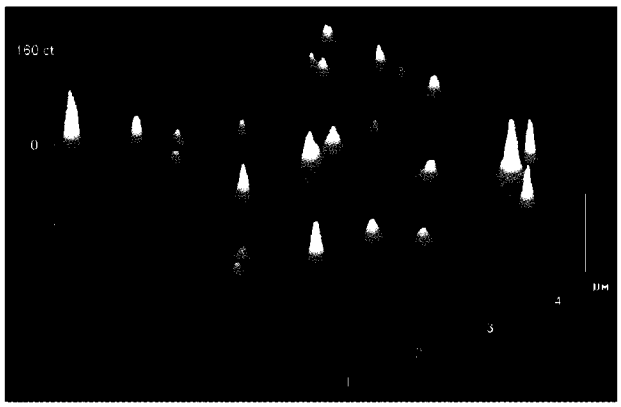

Fig. 3. Near-field fluorescence image (4.5 μm by 4.5 μm) of single oxazine 720 molecules dispersed on the surface of a poly(methylmethacrylate) film. Each subdiffraction peak (full width at half maximum, 100 nm) comes from a single molecule. Reproduced with permission from (*47*).

hertz in width at an optical frequency of hundreds of terahertz, a wealth of detailed information can be obtained, not only about the molecules and their interaction with the matrix, but also about their interaction with light, and about matrix dynamics. These three subjects are discussed hereafter.

The distribution of the line frequencies gives the inhomogeneous profile, free from vibrational contributions, whereas their lineshape directly yields the homogenous width, as was shown in several mixed molecular crystals (*13, 27*) (in contrast, ensemble measurements of the homogeneous width require elaborate nonlinear optical techniques). The fluorescence spectrum of a single molecule, as was demonstrated for terrylene in polyethylene (*28*), reflects its conformation and the symmetry of its specific nanoenvironment. Optical saturation, that is, the broadening and saturation of the line's intensity when the laser power is raised (*29*), may arise from the excited state lifetime or from the bottleneck effect of a dark state. In the latter case, dwelling of the molecule in the triplet manifold induces photon bunching, that is, a decay of the autocorrelation function of the fluorescence intensity. Bunching due to a triplet was first demonstrated with single pentacene molecules in *p*-terphenyl (*30*). While the molecule is in the triplet manifold, transitions among its electronic spin states can be driven by a microwave field. The ensuing change in average fluorescence rate (*31*), or in the statistics of the dark intervals (*32*) enables optically detected magnetic resonance (ODMR) at the single spin level. One step further, the nuclear magnetic resonance of a single proton can be induced, and detected through its effect on the ODMR line (*33*). Finally, the narrow line of a single molecule is extremely sensitive to weak external perturbations. An electric field, for example, leads to frequency shifts that can be quadratic or linear in field (*34*), depending on the local molecular symmetry.

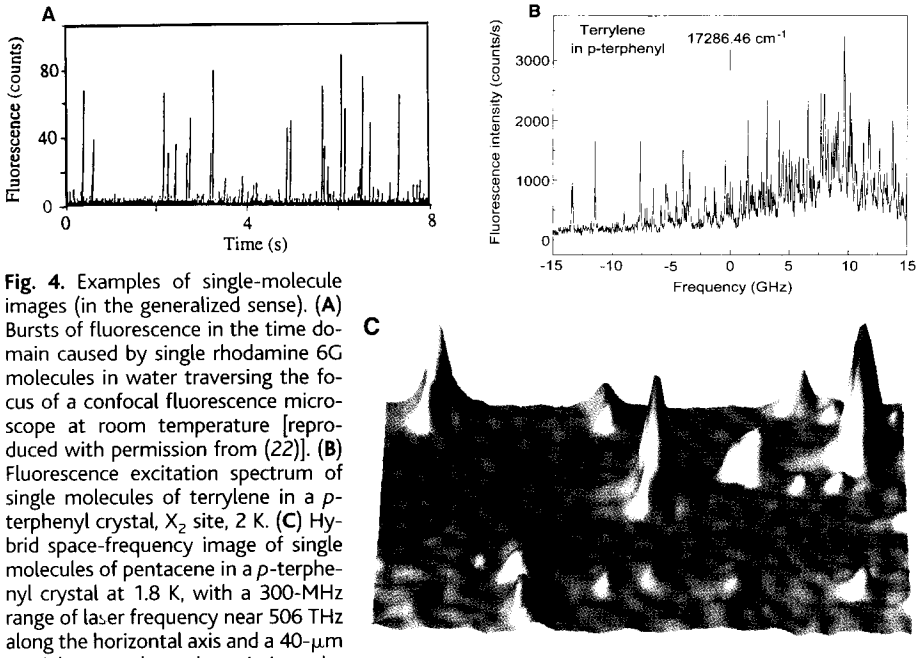

Fig. 4. Examples of single-molecule images (in the generalized sense). **(A)** Bursts of fluorescence in the time domain caused by single rhodamine 6G molecules in water traversing the focus of a confocal fluorescence microscope at room temperature [reproduced with permission from (*22*)]. **(B)** Fluorescence excitation spectrum of single molecules of terrylene in a *p*-terphenyl crystal, X_2 site, 2 K. **(C)** Hybrid space-frequency image of single molecules of pentacene in a *p*-terphenyl crystal at 1.8 K, with a 300-MHz range of laser frequency near 506 THz along the horizontal axis and a 40-μm spatial range along the axis into the page.

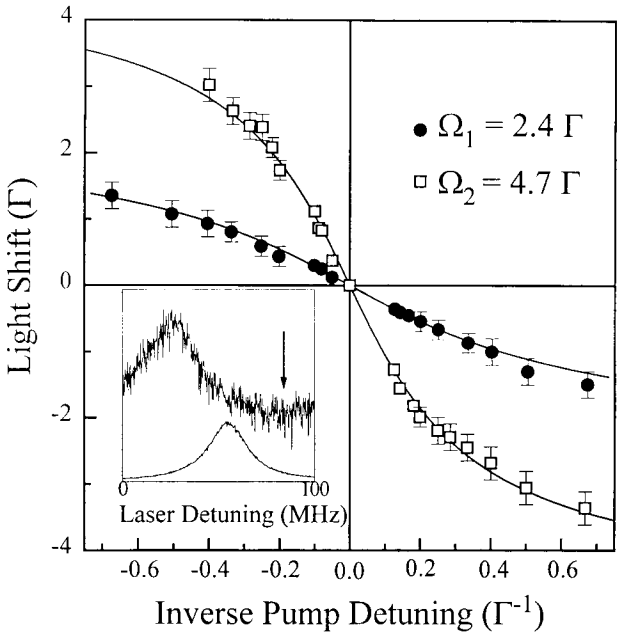

Fig. 5. Frequency shift of the excitation line of a single aromatic molecule in a molecular crystal at 2 K by a strong near-resonant pump beam. The light-induced shift is plotted as a function of the inverse of pump-molecule detuning for two values of the Rabi frequency Ω, in units of the linewidth Γ. The solid lines are fits from the simple model of an optical two-level system coupled to a resonant laser. (Inset) excitation spectrum without (lower trace) and with (upper trace) the pumping laser at the frequency shown by the arrow.

Much as the probing tip of a near-field microscope, a single molecule can respond to dynamical information about its solid environment because the resonance frequency of the molecule depends on the local strain. Again, the narrowness of the line leads to a high sensitivity of the molecule to movement at comparatively remote positions in the surroundings, and a weak back-action of the molecule on this movement. Fast fluctuations of the environment, for instance due to lattice phonons, lead to dephasing, that is to a broadening of the line. Under slow fluctuations of the transition frequency, on the other hand, the wandering of the line in frequency space can be followed in time. The associated phenomenon, called spectral diffusion, has been recorded for single pentacene molecules in a *p*-terphenyl crystal at 1.5 K (Fig. 6) (*38*). The frequency versus time trace in the lower panel is a "spectral trajectory" which cannot be directly observed in conventional ensemble studies. The sudden jumps have been interpreted as reorientations of the phenyl groups of nearby host molecules lying in domain walls (*39*). The residual dynamics of glasses down to very low temperatures are usually

interpreted in terms of low-energy defects, called two-level systems (*40*). One may picture these defects as small regions of the glass comprising several tens of atoms, and possessing two stable configurations with nearly the same energy, separated by a high barrier. Single molecules in polymers provide direct evidence for individual two-level systems in a glass. By studying the flip rate of a single two-level system as a function of temperature, one can attribute the flips to tunneling through the barrier. Tunneling can be assisted by the absorption or emission, or both, of one or two acoustic phonons, or can be activated, for example, by a quasi-local optical mode (*41*). The distributions of single-molecule linewidths in polymers such as poly(methylmethacrylate), poly(styrene) or poly(vinylbutyral) have been compared to spectral holeburning in the same systems (*42*). Detailed analysis of these distributions (*43*) and of large numbers of spectral trajectories may provide further tests of the standard model of two-level systems in amorphous materials.

Single-molecule optical studies at room temperature. The field of single-molecule optical research took an important critical step in 1993, with the first extended observations of single molecules at room temperature (*19*). [Single-molecule detection, that is, detection of the burst of light as a molecule diffuses through the focus of a laser beam, had been accomplished some years before (*24*); for a review of this area, see (*44*)]. To optimize emission from single molecules and to reduce scattering backgrounds, the experimenters spread the dye molecules on a dry surface and used near-field scanning optical microscopy to yield a spatial resolution of ~50 nm. Excitation with a subwavelength light source was produced by a pulled, metal-coated optical fiber tip (*19, 26, 45, 46*). For example, Fig. 3 shows a near-field fluorescence image of single oxazine 720 molecules dispersed on the surface of a poly(methyl methacrylate) film (*47*).

One concern in these near-field studies was the perturbation introduced in measurements of the emission lifetime produced by the proximity of the metal coating on the near-field tip (*46–48*). Subsequently, again by careful control of background by reduction of the excitation volume, both confocal microscopy (*22, 49*) and also wide-field epifluorescence microscopy (*50*) were shown to provide useful images of single dye molecules in solution, on surfaces, or in a levitated microdroplet (*51*). These diffraction-limited microscopic techniques have spatial resolution near $\lambda/2$, worse than the near-field method, but with the advantage of reduced complexity.

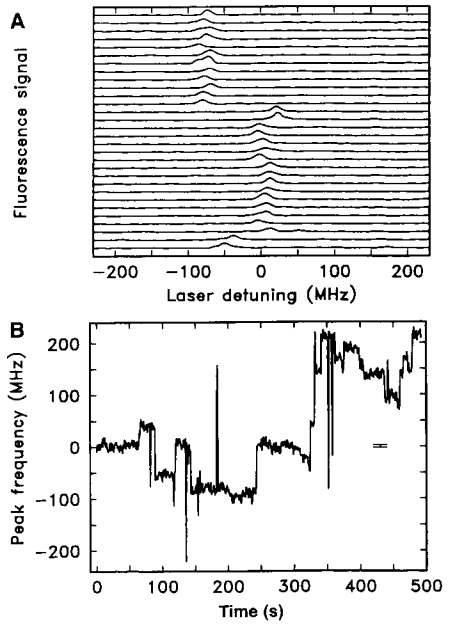

Fig. 6. Illustration of spectral jumps in the resonance frequency for a single pentacene molecule in a *p*-terphenyl crystal at 1.5 K. (**A**) A sequence of successive fluorescence excitation spectra each 2.5 s long spaced by 0.25 s; 0 MHz detuning corresponds to 592.546 nm. (**B**) Trend or trajectory of the resonance frequency versus time for the molecule in the upper panel. Reproduced with permission from (*29*).

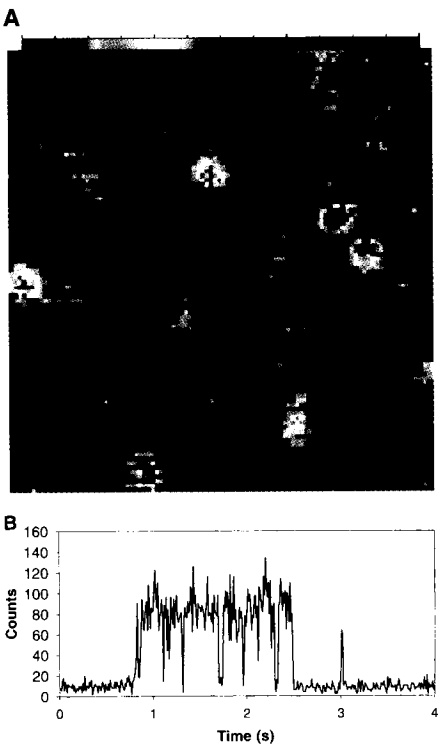

Fig. 7. (**A**) Confocal fluorescence image of single copies of the GFP mutant 10C (Ser65Gly/Val68Leu/Ser72Ala/Thr203Tyr; gift of R. Y. Tsien) embedded in a poly(acrylamide) matrix with polarized detection, scan rate of 10 ms per pixel. The average signal level in the fluorescence peaks was 10^4 counts/s for an incident intensity of 0.8 kW/cm^2. The color scale is shown for arbitrary units of fluorescence signal increasing from left to right. (**B**) Time-dependence of the spatially integrated emission from a single molecule, with a time resolution of 10 ms.

Two forces driving single-molecule research at room temperature are the simplicity compared to liquid helium temperatures and the large number of potential problems in physics, chemistry, and biology that may be explored. An area of currently expanding interest is the application of single-molecule techniques to the study of individual biomolecules in physiologically relevant environments. A key issue in observation of the same single molecule for an extended period of time in water at room temperature is control of Brownian motion; for example, a single small dye molecule can move roughly 30 μm rms for each second of observation. One way around this is to use a biological binding event to localize a labeled protein, and this approach has been applied to the observation of the single molecular motors myosin (*20*) and kinesin (*52*), reviewed in (*53*). Another approach involves entrapment of the single molecule or protein in water-filled pores of a poly(acrylamide) (*21*) or agarose (*47*) gel. A further solution involves attachment of a labeled protein of interest to a surface for visualization, such as the rotary motor, F_1–adenosine triphosphatase (*54*).

In an effort to obtain as much information as possible about the biological system under study, researchers have analyzed every aspect of the photons emitted, such as the location, polarization, time dependence, and spectral content. For example, by tracking the position of a single molecule emitter with time, two-dimensional diffusion of labeled phospholipids in membranes and lipid bilayers has been analyzed (*55*). Polarization studies report on the orientation of the fluorophore as a function of time, and such methods allow one to infer information about conformational changes of the nearby protein or oligonucleotide (*56*). A related method involves fluorescence resonance energy transfer (FRET) between a donor (emitter) molecule and a nearby acceptor (absorber) molecule, a technique that has already been widely used in biophysical studies (*57*). This technique, reviewed in (*58*), has the promise of providing more specific distance information in the 5- to 9-nm range, far below the optical diffraction limit, without requiring near-field optics.

The time dependence of the emission from a single biomolecule provides a wealth of additional information. First of all, in the nanosecond time regime, well-known time-correlated single-photon-counting methods allow direct measurement of the emission lifetime. In the case of a short 18-mer of DNA labeled with tetramethylrhodamine (TMR), researchers found biexponential decays with amplitudes varying from molecule to molecule, suggesting two local environments for the fluorophore: one corresponding to solvated TMR, and one to

TMR in close proximity to and quenched by the guanosine bases of the oligonucleotide (*59*). Similar lifetime studies have been performed on a variety of systems (*60*), including t-RNAs (*61*), bacterial light-harvesting complexes (*62*), and even single conjugated polymer molecules (*63*).

On longer time scales from microseconds to seconds, single-molecule emission has been used to report on a variety of additional time-dependent phenomena, from intersystem crossing dynamics, to diffusion, to chemical changes, to local configurational and environmental fluctuations. A related method for studying such effects, fluorescence correlation spectroscopy (FCS), has been applied to study time-dependent fluctuations, and this method works well when the fluctuation behavior is homogeneous from molecule to molecule (*64*). Here, however, we focus on single-molecule methods which observe the same single molecule for as long as possible until bleaching occurs. As a specific example, we consider single-molecule investigations of the well-known in situ reporter protein, the green fluorescent protein (GFP) of the jellyfish *Aequora victoria*, which has become a powerful tool for cellular biology. Its protein fold provides a scaffold for the formation of a bright emissive fluorophore formed entirely from the native amino acid residues of the protein (in the presence of oxygen). The utility of GFP as a cellular reporter of gene expression and the various mutants currently available have been recently reviewed (*65*). Mutants containing Ser65Gly or Ser65Thr constitute a broad class in which the phenolate anion form of the fluorophore is stabilized, and which can be conveniently pumped with Ar^+ ion laser lines (*66*). In 1997, the first observations of single copies of GFP were reported for this class (*67, 68*).

Figure 7 shows a confocal image of the emission from single copies of the GFP mutant 10C. A confocal image like this is obtained by scanning a ~400 nm diameter focal spot across the sample over a 10 μm by 10 μm range and collecting the emission through an aperture. Therefore, such an image is both a time record as well as a spatial record of the signal. One can clearly see relatively stable single molecules with little blinking during the scanning, as well as other single molecules which blink dramatically (lower center). Blinking effects were observed to occur even though continuous optical irradiation at 488 nm was present (*68*). Clearly, the molecule transforms between an emissive and a nonemissive state, but the exact mechanism underlying these changes is unknown at present. Such complex behavior can be analyzed by autocorrelation and on/off histograms of the time trajectory of the emission (*69*), which can then be contrasted with FCS data from even shorter time scales (*70*). Even longer lived dark states were observed, and optical irradiation at shorter wavelengths in the blue restored the original yellow-emissive form, like an optical switch (*68*).

The GFP case is but one example of a blinking or fluctuating process that has been observed in many systems at the single-molecule level (*71*). For example, the emission spectrum of single molecules at room temperature has been observed to fluctuate with time due to local environmental changes (*26, 72*). Similarly, conformational changes in single DNA molecules lead to fluctuations in emission (*60, 73*). The challenge remains to fully understand and interpret these phenomena. If the emission of the fluorescent label is strongly correlated with the biochemical state of an enzyme, then the time-dependence of the emission can report on the kinetics of the enzymatic cycle directly (*20, 74*).

Conclusion

The few examples mentioned here show how the high signal-to-noise ratios now available in single-molecule measurements allow for a wide variety of experiments in many fields. The main benefit of single-molecule isolation is the unraveling of ensemble averages. Totally new insight is thus gained into the structure and dynamics of condensed or living matter at nanometer scales, not only when inhomogeneities cause different molecules to behave in different ways, but also for identical nanosystems that fluctuate in time. Whereas time-resolved measurements on an ensemble demand synchronization of all subsystems, single-molecule experiments yield time-resolved information automatically.

The specific advantages of single-molecule studies will prove crucial in many fields, in applications as well as in fundamental investigations. In quantum optics, the isolation of a single quantum system greatly simplifies the description and understanding of its interaction with light. In recent years, single molecules have provided a wealth of new information about such fundamental processes as tunneling and activation in molecular crystals and polymers. But single molecules will also help solve difficult problems in physical chemistry at ambient conditions, such as surface-enhanced Raman scattering, adsorption and desorption of molecules on surfaces, dynamics in polymers and in other complex environments. For example, blinking was a quite unexpected effect that appears to be common to many single objects in various conditions. Finally, the scope and potential of single-molecule methods in biology cannot be overstated. Molecular heterogeneity, both in space and time, is quite characteristic of living matter, and single-molecule methods should find a large array of natural applications here. The many domains of biophysical chemistry which could benefit from single-molecule investigations range from protein folding and colocalization to the interactions between single biomacromolecules, from the mechanisms of molecular motors to the sequencing of single nucleic acid strands (*75*). The present issue vividly illustrates the wide scope and potential of single-molecule methods in this broad spectrum of scientific endeavor.

References and notes

1. R. P. Feynman, in *Miniaturization*, H. D. Gilbert, Ed. (Reinhold, New York, 1961).
2. G. Binnig and H. Rohrer, *Rev. Mod. Phys.* **59**, 615 (1987).
3. G. Binnig, C. F. Quate, C. Gerber, *Phys. Rev. Lett.* **56**, 930 (1986); D. Sarid, *Scanning Force Microscopy* (Oxford Univ. Press, New York, 1994).
4. W. M. Itano, J. C. Bergquist, D. J. Wineland, *Science* **237**, 612 (1987); F. Diedrich, J. Krause, G. Rempe, M. O. Scully, H. Walther, *IEEE J. Quantum Electron.* **24**, 1314 (1988); H. Dehmelt, W. Paul, N. F. Ramsey, *Rev. Mod. Phys.* **62**, 525 (1990).
5. T. Basché, S. Kummer, C. Bräuchle, *Nature* **373**, 132 (1995).
6. W. E. Moerner and T. Basché, *Angew. Chem. Int. Ed. Engl.* **32**, 457 (1993); W. E. Moerner, *Science* **265**, 46 (1994); *Acc. Chem. Res.* **29**, 563 (1996).
7. M. Orrit, J. Bernard, R. Brown, B. Lounis, in *Progress in Optics*, E. Wolf, Ed. (Elsevier, Amsterdam, 1996), vol. 35, pp. 61–144.
8. T. Plakhotnik, E. A. Donley, U. P. Wild, *Annu. Rev. Phys. Chem.* **48**, 181 (1997).
9. T. Basché, W. E. Moerner, M. Orrit, U. P. Wild, Eds., *Single Molecule Optical Detection, Imaging, and Spectroscopy* (Verlag-Chemie, Weinheim, Germany, 1997).
10. S. Nie and R. N. Zare, *Annu. Rev. Biophys. Biomol. Struct.* **26**, 567 (1997).
11. X. S. Xie and J. K. Trautman, *Annu. Rev. Phys. Chem.* **49**, 441 (1998).
12. W. E. Moerner and L. Kador, *Phys. Rev. Lett.* **62**, 2535 (1989).
13. M. Orrit and J. Bernard, *ibid.* **65**, 2716 (1990).
14. R. Y. Tsien and A. Waggoner, in *Handbook of Biological Confocal Microscopy*, J. B. Pawley, Ed. (Plenum, New York, ed. 2, 1995), pp. 267–279.
15. A. Gruber *et al.*, *Science* **276**, 2012 (1997).
16. D. Gammon *et al.*, *ibid.* **277**, 85 (1997); S. A. Empedocles, M. G. Bawendi, *ibid.* **278**, 2114 (1997).
17. M. J. Bruchez, M. Moronne, P. Gin, S. Weiss, A. P. Alivisatos, *ibid.* **281**, 2013 (1998); W. C. W. Chan and S. Nie, *ibid.*, p. 2016.
18. K. K. Rebane, *Chem. Phys.* **189**, 139 (1994); W. E. Moerner, R. M. Dickson, D. J. Norris, *Adv. At. Mol. Opt. Phys.* **38**, 193 (1997).
19. E. Betzig and R. J. Chichester, *Science* **262**, 1422 (1993).
20. T. Funatsu, Y. Harada, M. Tokunaga, K. Saito, T. Yanagida, *Nature* **374**, 555 (1995).
21. R. M. Dickson, D. J. Norris, Y.-L. Tzeng, W. E. Moerner, *Science* **274**, 966 (1996).
22. S. Nie, D. T. Chiu, R. N. Zare, *ibid.* **266**, 1018 (1994).
23. F. Güttler, T. Irngartinger, T. Plakhotnik, A. Renn, U. P. Wild, *Chem. Phys. Lett.* **217**, 393 (1994).
24. E. B. Shera, N. K. Seitzinger, L. M. Davis, R. A. Keller, S. A. Soper, *ibid.* **174**, 553 (1990).
25. U. Mets and R. Rigler, *J. Fluorescence* **4**, 259 (1994).
26. J. K. Trautman, J. J. Macklin, L. E. Brus, E. Betzig, *Nature* **369**, 40 (1994).
27. W. E. Moerner and W. P. Ambrose, *Phys. Rev. Lett.* **66**, 1376 (1991).
28. P. Tchénio, A. B. Myers, W. E. Moerner, *Chem. Phys. Lett.* **213**, 325 (1993).
29. W. P. Ambrose, T. Basché, W. E. Moerner, *J. Chem. Phys.* **95**, 7150 (1991).
30. J. Bernard, L. Fleury, H. Talon, M. Orrit, *ibid.* **98**, 850 (1993).
31. J. Köhler *et al.*, *Nature* **363**, 242 (1993); J. Wrachtrup, C. von Borczyskowski, J. Bernard, M. Orrit, R. Brown, *ibid.*, p. 244.
32. A. C. J. Brouwer, E. J. J. Groenen, J. Schmidt, *Phys. Rev. Lett.* **80**, 3944 (1998).
33. J. Wrachtrup, A. Gruber, L. Fleury, C. von Borczyskowski, *Chem. Phys. Lett.* **267**, 179 (1997).

34. U. P. Wild, F. Güttler, M. Pirotta, A. Renn, *ibid.* **193**, 451 (1992); M. Orrit, J. Bernard, A. Zumbusch, R. I. Personov, *ibid.* **196**, 595 (1992).
35. T. Basché, W. E. Moerner, M. Orrit, H. Talon, *Phys. Rev. Lett.* **69**, 1516 (1992).
36. T. Plakhotnik, D. Walser, M. Pirotta, A. Renn, U. P. Wild, *Science* **271**, 1703 (1996).
37. P. Tamarat *et al.*, *Phys. Rev. Lett.* **75**, 1514 (1995); C. Brunel, B. Lounis, P. Tamarat, M. Orrit, *ibid.* **81**, 2679 (1998).
38. W. P. Ambrose and W. E. Moerner, *Nature* **349**, 225 (1991).
39. P. D. Reilly and J. L. Skinner, *J. Chem. Phys.* **102**, 1540 (1995).
40. W. A. Phillips, Ed., *Amorphous Solids: Low-Temperature Properties* (Springer, Berlin, 1981).
41. A. Zumbusch, L. Fleury, R. Brown, J. Bernard, M. Orrit, *Phys. Rev. Lett.* **70**, 3584 (1993).
42. B. Kozankiewicz, J. Bernard, M. Orrit, *J. Chem. Phys.* **101**, 9377 (1994).
43. E. Geva and J. L. Skinner, *J. Phys. Chem. B* **101**, 8920 (1997).
44. R. A. Keller *et al.*, *Appl. Spectrosc.* **50**, 12A (1996).
45. X. S. Xie and R. C. Dunn, *Science* **265**, 361 (1994).
46. W. P. Ambrose, P. M. Goodwin, J. C. Martin, R. A. Keller, *ibid.*, p. 364.
47. X. S. Xie, *Acc. Chem. Res.* **29**, 598 (1996).
48. J. K. Trautman and J. J. Macklin, *Chem. Phys.* **205**, 221 (1996); R. X. Bian, R. C. Dunn, X. S. Xie, P. T. Leung, *Phys. Rev. Lett.* **75**, 4772 (1995).
49. M. Eigen and R. Rigler, *Proc. Natl. Acad. Sci. U.S.A.* **91**, 5740 (1994).
50. J. J. Macklin, J. K. Trautman, T. D. Harris, L. E. Brus, *Science* **272**, 255 (1996).
51. M. D. Barnes, W. B. Whitten, J. M. Ramsey, *Anal. Chem.* **67**, A418 (1995).
52. R. D. Vale, *et al.*, *Nature* **380**, 451 (1996).
53. A. D. Mehta, M. Reif, J. A. Spudich, D. A. Smith, R. M. Simmons, *Science* **283**, 1689 (1999).
54. H. Noji, R. Yasuda, M. Yoshida, K. J. Kinosita, *Nature* **386**, 299 (1997).
55. T. Schmidt, G. J. Schutz, W. Baumgartner, H. J. Gruber, H. Schindler, *Proc. Natl. Acad. Sci. U.S.A.* **93**, 2926 (1996).
56. T. Ha, T. Enderle, D. S. Chemla, P. R. Selvin, S. Weiss, *Phys. Rev. Lett.* **77**, 3979 (1996); T. Ha, J. Glass, T. Enderle, D. S. Chemla, S. Weiss, *ibid.* **80**, 2093 (1998).
57. L. Stryer, *Annu. Rev. Biochem.* **47**, 819 (1978); B. W. Van der Meer, G. Coker III, S.-Y. Chen, *Resonance Energy Transfer: Theory and Data* (VCH, New York, 1994).
58. S. Weiss, *Science* **283**, 1676 (1999).
59. L. Edman, U. Mets, R. Riger, *Proc. Natl. Acad. Sci. U.S.A.* **93**, 6710 (1996).
60. C. Eggeling, J. R. Fries, L. Brand, R. Gunther, C. A. M. Seidel, *ibid.* **95**, 1556 (1998).
61. Y. Jia *et al.*, *ibid.* **94**, 7932 (1997).
62. M. A. Bopp, Y. Jia, L. Li, R. J. Cogdell, R. M. Hochstrasser, *ibid.*, p. 10630.
63. D. A. VanDen Bout *et al.*, *Science* **277**, 1074 (1997).
64. E. L. Elson and D. Magde, *Biopolymers* **13**, 1 (1974); D. L. Magde, E. L. Elson, W. W. Webb, *ibid.* **13**, 29 (1974); R. Rigler, *J. Biotechnol.* **41**, 177 (1995).
65. R. Y. Tsien, *Annu. Rev. Biochem.* **67**, 509 (1998).
66. M. Ormo *et al.*, *Science* **273**, 1392 (1996); J. Llopis, J. M. McCaffery, A. Miyawaki, M. G. Farquhar, R. Y. Tsien, *Proc. Natl. Acad. Sci. U.S.A.* **95**, 6803 (1998).
67. D. W. Pierce, N. Hom-Booher, R. D. Vale, *Nature* **388**, 338 (1997).
68. R. M. Dickson, A. B. Cubitt, R. Y. Tsien, W. E. Moerner, *ibid.*, p. 355.
69. W. E. Moerner, E. J. P. Peterman, S. Brasselet, S. Kummer, R. M. Dickson, *Bioimaging*, in press.
70. U. Haupts, S. Maiti, P. Schwille, W. W. Webb, *Proc. Natl. Acad. Sci. U.S.A.* **95**, 13573 (1998).
71. W. E. Moerner, *Science* **277**, 1059 (1997).
72. H. P. Lu and X. S. Xie, *Nature* **385**, 143 (1997).
73. S. Wennmalm, L. Edman, R. Rigler, *Proc. Natl. Acad. Sci. U.S.A.* **94**, 10641 (1997).
74. H. P. Lu, L. Xun, X. S. Xie, *Science* **282**, 1877 (1998).
75. P. M. Goodwin *et al.*, *Nucleosides Nucleotides* **16**, 543 (1997).
76. W.E.M. was supported in part by NSF grant DMR-9612252. We thank S. Brasselet for providing data for Fig. 7 and R. Y. Tsien for the gift of the GFP mutant.

COVER Optical images of single molecules. Clockwise from upper left. Frequency-space: pentacene in *p*-terphenyl at 2 kelvin (K). Confocal: protein kinase A regulatory subunit in agarose gel, 295 K (room temperature). Total internal reflection: green fluorescent protein in polyacrylamide gel, 295 K. Far-field epifluorescence: terrylene in *p*-terphenyl, 2 K. Special section topics begin on p. 1667. [Images: W. E. Moerner, W. P. Ambrose, S. Brasselet, J. Deich, R. M. Dickson, D. J. Norris, S. S. Taylor]